Precise modulation of drug release from emulsions via modification of Pickering particles properties: a computational study using population balance equations

Chemical Engineering Science 337 (2027) 124620

Contents lists available at ScienceDirect

Chemical Engineering Science

journal homepage: www.elsevier.com/locate/ces

Precise modulation of drug release from emulsions via modification of Pickering particles properties: a computational study using population balance equations☆

Pierfrancesco Latorre, Antonio Buffo *, Elena Simone *

Department of Applied Science and Technology (DISAT), Politecnico di Torino, Torino 10129, Italy

ARTICLE INFO

Keywords:
Pickering
Population balance equations
Drug release

ABSTRACT

Pickering emulsions, stabilized by solid particles at the interface between continuous and disperse phase, have gained attention due to their advantages over traditional surfactant-stabilized systems. Crystalline particles are promising Pickering materials as their interfacial activity can be controlled by changing crystal properties such as size, shape and polymorphism. Pickering particles can play a crucial role in modulating the release of active ingredients (AI) encapsulated in the dispersed phase. In fact, by controlling the dissolution of Pickering particles, which act as physical barrier to the AI diffusion, it is possible to modulate the release of the AI itself. Hence, enabling stimuli-responsive and/or prolonged release. To gain deeper insight into this release mechanism, we developed a theoretical model that integrates population balance equations (PBE) to describe Pickering particle dissolution, and Fick's law of diffusion to describe the release of AI from the disperse phase. The PBEs were solved using the High-Resolution Finite Volume method, ensuring accurate numerical representation of dissolution dynamic. Based on experimental observations reported in the literature, our model can capture the evolution of AI concentration in the dispersed and continuous phase, and it can be used to identify how particle population properties, especially particle size and shape distributions, influence release behavior, thereby supporting formulation screening toward specific AI release profiles.

1. Introduction

Emulsions are biphasic systems consisting of mixtures of two or more immiscible liquids; these are temporarily stabilized into a continuous and a dispersed phase by the presence of interfacially actives compounds (e.g., surfactants, amphiphilic molecules). In recent years there has been a growing interest in a specific class of multiphase formulations known as Pickering systems (Pickering, 1907), which are stabilized by solid particles rather than conventional surfactants. The growing popularity of Pickering emulsions (Ribeiro et al., 2023) is primarily due to their broad range of applications (de Carvalho-Guimarães et al., 2022; Gonzalez Ortiz et al., 2020) spanning pharmaceuticals (Frelichowska et al., 2009; da Ferreira et al., 2022; Shah et al., 2021), food (Zhang et al., 2024; Ghosh and Rousseau, 2011; Liu et al., 2019) and cosmetics (Miller et al., 2001; Hu et al., 2022), among others. Unlike conventional emulsions, where stability is achieved through the decrease in surface tension determined by molecular surfactants, Pickering emulsions are stabilized by solid particles that adsorb more strongly than surfactants at the liquid–liquid interface, preventing coalescence of the dispersed droplets. This stabilization mechanism offers three main advantages compared to traditional stabilizers: i) enhanced stability, as the solid particles adsorb irreversibly at the interface, more strongly than surfactants; ii) solid particles may also provide additional functional benefits, including improved biocompatibility, environmental sustainability, and reduced toxicity compared to conventionally synthesized surfactants (de Carvalho-Guimarães et al., 2022; Yang et al., 2017; Xia et al., 2021); iii) the possibility to engineer Pickering particles with specific properties (e.g., size, shape, wettability), enabling the design of tailored, function-specific multiphase systems.

Particles properties have been found to play a huge role in the stability and in the resulting microstructure of the Pickering emulsions obtained. Particularly, wettability (Binks and Lumsdon, 2000), particle size (Qi et al., 2014), shape (Madivala et al., 2009) and concentration (Aveyard et al., 2003; Frungieri and Briesen, 2023) strongly affect the

☆ This article is part of a special issue entitled: 'PBM 2025 ? Ramki Tribute' published in Chemical Engineering Science.

* Corresponding authors.
E-mail addresses: antonio.buffo@polito.it (A. Buffo), elena.simone@polito.it (E. Simone).

https://doi.org/10.1016/j.ces.2026.124620
Received 21 December 2025; Received in revised form 17 April 2026; Accepted 8 July 2026
Available online 9 July 2026

functionality and microstructure of Pickering emulsions.

The role of stabilizing agent in Pickering systems can be played by a wide variety of solid particles (Yang et al., 2017; Xia et al., 2021): hydroxyapatite crystals have been extensively used in the formation of Pickering emulsions due to their excellent surface activity, also silica particles have been used as they are convenient and their surface can be chemically modified, clay particles are also a popular choice of Pickering stabilizer, together with magnetic nanoparticles, chitosan, cyclodextrin, carbon nanotubes, starch granules, proteins and many more (Yang et al., 2017; Xia et al., 2021). Chen et al. (Chen et al., 2020) also present the use of fat crystals as Pickering particles in water-in-oil emulsions.

Small organic molecule crystals are a particularly promising Pickering stabilizer; they present many advantages compared to other food-grade Pickering systems (e.g., proteins, zein, crystalline cellulose), such as: (1) they are fully biocompatible, non-toxic and, in some cases, they provide health benefits (e.g., curcumin, quercetin) (Zembyla et al., 2018), (2) they can be extracted from plants, seeds or milk without the use of organic chemicals and using green technologies (e.g. supercritical CO_2) and (3) they can be easily modified in terms of size, shape and internal crystalline structure (polymorphism) by controlling the conditions in which these crystals are nucleated and grown (Del Duca et al., 2024).

Among the many potential applications of Pickering emulsions, heavily linked to the particles properties, one of the most promising, and the focus of the present study is the controlled, stimuli-responsive delivery of active ingredients (AIs) encapsulated in the dispersed phase. Recent studies have shown the possibility of engineering Pickering particles for the encapsulation and controlled release of AIs (Hiranphinyophat et al., 2021; Lan et al., 2007; Li et al., n.d.; Low et al., 2019; Mwangi et al., 2020; Raju et al., 2018; Sanyal et al., 2011; Shirjandi et al., 2022; Tikekar et al., 2013; Zhao et al., 2018). Different strategies have been investigated over the years (Mwangi et al., 2020); for example, Li et al. (n.d.) have used cellulose nanocrystals allomorph II (CNCs), with a characteristic cylindrical elongated rod or needle-like shape, to modulate the release of ibuprofen from CNC-stabilized emulsions. Also, Hiranphinyophat et al. 2021 (Hiranphinyophat et al., 2021) investigated the use of modified cellulose nanocrystals as stabilizers for bifonazole loaded Pickering emulsions, to be used for topical drug delivery. Another strategy was proposed by Low et al. (Low et al., 2019; Low et al., 2018) who designed magnetic cellulose nanocrystals able to respond to magnetic stimuli and enable AI release. pH-responsive Pickering systems were developed for application in both the pharmaceutical and cosmetic field (Lan et al., 2007; Shirjandi et al., 2022); Tikekar et al. (Tikekar et al., 2013) have studied the release of curcumin from Pickering emulsions upon oral administration, observing the strong effect of pH on the curcumin release rate. Another study on the influence of pH was carried out by Raju et al (Raju et al., 2018) who have worked on chitosan-based Janus Pickering particles used to stabilize emulsions with olive and silicone oil. Temperature changes have been investigated as stimulus to trigger the release from Pickering emulsions; Sanyal et al. (Sanyal et al., 2011) designed thermal-responsive composite nanoparticles.

All the aforementioned studies are experimental and apply trial-and-error approaches to optimize particle properties and emulsion microstructure in order to obtain the desired stimuli-responsive formulation. Rigorous theoretical models that describe the different mechanisms of stimuli-triggered AI release from Pickering systems are currently missing, despite their large potential benefits for effective formulation design and optimization.

The aim of this work is to fill this knowledge gap and develop a theoretical model capable of realistically describing the release mechanism of an AI from within dispersed phase droplets. Our proposed model can help researchers in the field to understand their AI release mechanism, highlighting the link between Pickering particle dissolution and AI diffusion rate. Furthermore, the model can support the formulation of Pickering emulsions by identifying how particle population properties, especially particle size and shape distributions, together with the particle dissolution behavior, influence AI release. This information can guide the experimental screening of formulations aimed at specific release behaviors. The description of the release of encapsulated AIs in Pickering emulsions is achieved by solving a Population Balance Equation (PBE) that incorporates a dissolution term for the crystal population located on the droplet surface. The PBE is combined with mass balance equations for the AI in the continuous and disperse phases. At this stage, the proposed model should be regarded primarily as a framework aimed for describing how Pickering particle dissolution modifies interfacial coverage and, in turn, active ingredient release, with particular emphasis on the role of the Pickering particle properties in the formulation design. For this reason, the present work focuses on the evolution of a single Pickering droplet. It is worth noting that quantitative predictive use for a specific Pickering formulation would require calibration and validation against dedicated experiments, which are currently not available in the literature in a sufficiently complete form, since published studies generally do not report particle size distribution, interfacial coverage, particle dissolution, and active ingredient release under controlled conditions. Additionally, the single-droplet formulation makes direct experimental validation particularly challenging.

Population balance modelling has already been applied to several problems related to Pickering or particle-stabilized systems, including emulsion polymerization, droplet size evolution, coalescence and breakup, and surface coverage development during emulsion preparation (Brunier et al., 2022; Klink et al., 2011; Brunier, 2015; Frungieri and Briesen, 2023; Röhl et al., 2023). At the same time, numerous works are available in the literature regarding Population Balance modelling of crystallization processes (Bosetti and Mazzotti, 2020; Dighe et al., 2019; Gagliardi and Pierre-Louis, 2018; Maharana et al., 2023; Pohar and Likozar, 2014; Swapna Reddy et al., 2023) as well as crystal dissolution in different environmental settings (Barlow et al., 2022; Chaudhury et al., 2013; Plath et al., 2024; Shan et al., 2002; Lasaga and Lüttge, 2003). Recently, the effect of crystal size on dissolution rate has also been investigated with a Monte Carlo model (Briese et al., 2017).

To the authors' knowledge, however, a population balance-based model describing the dissolution of Pickering particles at the droplet interface and its coupling with the release of an active ingredient from the dispersed phase has not yet been reported. In this sense, the novelty of the present work lies in the coupling among interfacial particle dissolution, evolution of surface coverage, and active ingredient diffusion during the post-formation release stage to describe the delivery mechanism of Pickering systems.

This paper is divided in a first section describing the constitutive equations of the model and the initial hypothesis and boundary conditions. The second section provides details on the method used for the numerical solution of the equations. Then, a detailed description of the conditions used for simulations is provided, followed by a section showing the simulations results. Conclusions and possible future expansions and applications of the developed model are then illustrated.

2. Model description

Our model describes the release of an AI encapsulated within a single Pickering droplet upon administration; this can be caused by a dilution of the continuous phase and is usually accompanied by a change in temperature or pH, which alters crystal solubility in the continuous phase, inducing the dissolution and detachment of Pickering particles from the interface. This, in turn, enables the diffusion of AI from the droplet to the surrounding environment. The single-droplet formulation presented here is intended to isolate the local coupling between particle dissolution, interfacial coverage evolution, and AI diffusion. As such, it does not account for droplet–droplet interactions or for differences among droplets within a real emulsion. It is worth noting that a change

in contact angle might also be triggered by administration; however, for micron-sized crystalline Pickering particles such change does not usually significantly affect interfacial stabilization (Del Duca et al., 2024). Hence, for simplicity, the model presented here treats the contact angle as fixed at its post-stimulus value. This assumption avoids the introduction of a function to describe changes in wetting behavior, but it may limit applicability in systems where particle exposure to the continuous phase changes significantly over time.

The dissolution of the Pickering particles adsorbed at the interface increases the mass transfer area available for AI diffusion. Hence, by appropriately changing the kinetics of Pickering particle dissolution it is possible to modulate the AI release rate. Such kinetics can be modulated by changing the particle size and shape distributions, or the interfacial particle concentration (e.g., multiple layers) (Dan, 2016).

Additionally, the solubility of Pickering particles in the continuous phase can be modified by using different polymorphs (Abdul Mudalip et al., 2018; Lee et al., 2025). All these particle properties that can affect the dissolution rate of Pickering particles will be investigated in this study.

We assume our Pickering particle being of a rod shape, exemplified in Fig. 1, with one characteristic size L being larger than the other two assumed equal for simplicity, with size W. Thus, it is possible to define the particle aspect ratio ϕ as follows:

$$\phi = L/W \tag{1}$$

From other works and from previous experimental studies on similar systems, we found that it is not uncommon to have Pickering systems with particles of similar shape distributed over their characteristic size L, but with similar aspect ratio ϕ, making it reasonable to assume with a mean aspect ratio (Del Duca et al., 2024; Lee et al., 2025; Liang et al., 2017; Madivala et al., 2009; Lou et al., 2016).

This aspect led us to consider the following mono-dimensional population balance equation:

$$\frac{\partial n(L,t)}{\partial t} + \frac{\partial (G(L,t)n(L,t))}{\partial L} = 0 \tag{2}$$

where the quantity $n(L,t)dL$ represents the expected number of particles of characteristic size L per unit area at the droplet interface at time t. The first left hand side term is the accumulation term, while the second term has the form of a convective term, where $G(L,t)$ is the dissolution rate, a function of the particle size L and time t. It can be noted that the particle aspect ratio ϕ does not appear in Eq. (2) since it is assumed equal for all particles. For particles distributed also over the aspect ratio ϕ, it would be more appropriate to write a more rigorous bi-dimensional population balance equation, but the lack of reliable bi-dimensional dissolution models (i.e., $G(L,\phi)$) sets this last aspect out of the scope of this work.

It is worth noting that aggregation may affect interfacial coverage and dissolution kinetics. Particle aggregation can occur during the adsorption process, when the emulsion is prepared, especially if the particle-to-droplet size ratio is high or when interfacial crowding

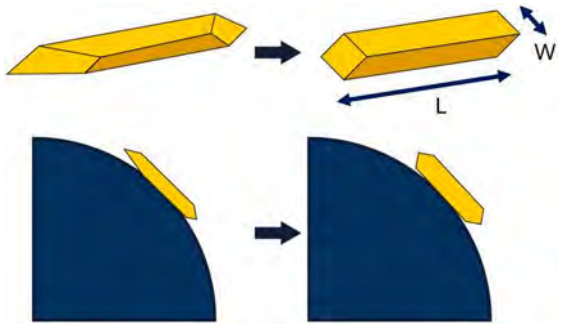

Fig. 1. Approximation of the shape of the crystals and their arrangement at the droplet surface.

becomes significant (Madivala et al., 2009; Frungieri and Briesen, 2023; Madivala et al., 2009; Lou et al., 2016). In the model presented here, particle aggregation is neglected, under the assumption of low concentrations of Pickering particles and low to moderate particle-to-droplet size ratios. More precisely, the present model formulation is intended for conditions in which interfacial shielding is mainly determined by individually adsorbed particles, rather than by aggregates or multilayer structures. Nevertheless, aggregation could in principle be implemented in the model; for example, the initial particle size distribution and the particle shape factors could be adapted to address the presence of crystal agglomerates.

The dissolution term $G(L,t)$ that appears in Eq. (1) must have a negative sign, expressing the reduction of the size of the Pickering crystals over time. The vast majority of the dissolution models available in the literature expresses this rate as function of the undersaturation of the system:

$$S(t) = C_{solub}/C_p(t) \tag{3}$$

where C_{solub} is the solubility of the Pickering particles in the continuous, and it is a function of the thermodynamics state of the system (e.g., temperature, composition of the continuous phase), and $C_p(t)$ is the actual solute concentration upon dissolution of the Pickering particles in the continuous phase. It is worth pointing out that our model considers the Pickering particles insoluble in the dispersed phase (this may also be due to the fact that the dispersed phase is already saturated with the Pickering compound).

A typical expression used to express dissolution as function of undersaturation is a power-law, as the one formulated by Bosetti et al. (Bosetti and Mazzotti, 2020) and by Lifshitz et al. (Lifshitz and Slyozov, 1961). For the current work, we adopted a simplified version of such expression (Bosetti and Mazzotti, 2020; Myerson et al., 2019):

$$G(L,t) = k_g(S(t) - 1)^g \tag{4}$$

where g is an exponent that typically ranges from 1 and 2 (Myerson et al., 2019), with $g = 1$ representing a mass-transfer limited process. Following this assumption, k_g is often treated as a constant parameter fitted with experimental data, especially in well mixed conditions. This leads to an equal dissolution rate for all the particles. Such a size-independent kinetic expression should be interpreted as a first-order approximation. It may not be accurate for dissolution mechanisms in which the rate depends strongly on particle size, morphology, or on differences in the area of the particle exposed to the continuous phase. However, for the relatively narrow particle size distributions considered here, it represents a reasonable approximation. In any case, the model could be easily modified to implement a different expression for k_g. For a mass-transfer limited dissolution, Eq. (4) further simplifies to the following expression:

$$G(t) = k_g(S(t) - 1) \tag{5}$$

To evaluate the undersaturation ratio $S(t)$, the knowledge of the solute concentration of the Pickering particle compound in the continuous phase $C_b(t)$ over time is needed. This time evolution has been calculated through the following expression:

$$\frac{dC_p}{dt} = \frac{k_v\rho}{M_w V_c}\frac{d}{dt}\left(\int_0^{+\infty} n(L,t)L^3 dL\right) = \frac{k_v\rho}{M_w V_c}\int_0^{+\infty}\frac{\partial n(L,t)}{\partial t}L^3 dL \tag{6}$$

where V_c is the volume of the continuous phase, M_w is the molar mass of the Pickering particles species and the term $\left(\int_0^{+\infty}\frac{\partial n(L,t)}{\partial t}L^3 dL\right)$ represents the variation in time of the moment of third order of the distribution, which multiplied by the volumetric shape factor k_v (equal to $\frac{1}{\phi^2}$ for rectangular rods) gives the total variation of the crystal volume in our system. The factor k_v is a parameter that can be changed to accommodate different crystal shapes. It must be noted that Eq. (6) has been

written with an underlying hypothesis, namely that only one face of the Pickering particles is in contact with the droplet surface, while all the other faces are surrounded by the continuous phase; this is compatible with a three phase contact angle between continuous, disperse and solid phases equal to 90 degrees. Fig. 1 shows the specific assumption adopted in this work. However, this assumption may not always be physically accurate; in fact, depending on the affinity of the particles with the surrounding phases, they may establish a different contact angle with the droplet, thereby changing the percentage of particles' area wetted by the two phases.

Nevertheless, the contact angle can be difficult to evaluate in the case of real particles, due to their superficial roughness and anisotropy (Del Duca et al., 2024). Despite the complexity of the phenomenon, the model presented here could still treat the effect of different contact angles through a parametrized description, allowing the portion of the particle available for dissolution (i.e., immersed in the continuous phase) to depend on the contact angle. In the specific case presented here, a 90° contact angle leads to an areic shape factor k_a equal to $1/\phi$, indicating that only one face is in contact with the droplet, while the other five are immersed in the continuous phase. A different particle shape and contact angle would lead to different values of the shape factors k_v and k_a, giving to the model some flexibility in representing different interfacial configurations. However, in the present work these effects are not allowed to evolve dynamically in time, and this represents a further simplifying assumption of the current model formulation.

It is then possible to calculate the total area of the droplet surface that is occupied by the Pickering particles using the following expression, using the areic shape factor k_a:

$$S_{cry}(t) = \int_{L_0}^{+\infty} k_a n(L,t) L^2 dL \tag{7}$$

which can be seen as a quantity proportional to the moment of order 2 with respect to the particle size distribution. The extent of droplet coverage by crystals is usually referred to as the covering fraction f, defined as the ratio between the total surface area occupied by the Pickering particles and the droplet surface area:

$$f(t) = S_{cry}(t)/S_d \tag{8}$$

where S_{drop} can be calculated in the following way, assuming a spherical shape

$$S_d = \pi d_d^2 \tag{9}$$

When the incapsulated active ingredient is considered, it is possible to write the following equations to evaluate the diffusion from the droplet to the continuous phase, considering the mass transfer through the droplet interface:

$$\frac{dC_{AI,d}}{dt} = -\left(\frac{P}{k_d} + \frac{1}{k_c}\right)^{-1} (PC_{AI,d} - C_{AI,c})A \tag{10}$$

$$\frac{dC_{AI,c}}{dt} = \left(\frac{P}{k_d} + \frac{1}{k_c}\right)^{-1} (PC_{AI,d} - C_{AI,c})A \tag{11}$$

where $C_{AI,d}$ and $C_{AI,c}$ are respectively the concentration of the active ingredient in the droplet and in the continuous phase, $\left(\frac{P}{k_d} + \frac{1}{k_c}\right)^{-1}$ is the overall mass transfer coefficient, k_d and k_c are respectively the mass transfer coefficient in the droplet and in the continuous phase, P is the partition coefficient, defined as $P = \frac{C_{AI,d}}{C_{AI,c}}$, and A is the interfacial area between the droplet and the continuous phase. The partition coefficient plays an important role, as it is needed to correctly take into consideration the relative affinity of the AI to the two phases and to estimate the driving force for the diffusion of the AI from the droplet to the continuous phase. In the case of oral administration, enzymatic digestion of the disperse oil phase would have an effect on the rate of release of AI. A modified version of our model, including the effect of lipase is presented in the Supporting Information of this paper (Fig. S1).

It should be highlighted that the link between the population balance model for the Pickering particle distribution and the AI balance is through the interfacial area term, that can be written in the following way:

$$A(t) = S_d - S_{cry}(t) = S_d(1 - f(t)) \tag{12}$$

As it is possible to see from Eq. (12), the interfacial area is initially a fraction of the total droplet external surface, since initially it is covered by the Pickering particles. As soon as the dissolution of the Pickering particles starts, the covering fraction $f(t)$ decreases evolving towards a clean surface, when no Pickering particles are at the droplet surface (namely when $f(t) = 0$).

It should be noted that Eqs. (10) and (11) are derived using the two-film theory (Bird et al., 2002), which assumes that the interface does not change with time, this being an essential condition to express the interfacial molar flux in terms of a driving force and an overall mass transfer coefficient. Although in our case the interfacial area changes with time, following the evolution of the covering fraction $f(t)$, we deliberately retain the model simplicity for the interfacial molar flux, introducing the dependence of time only in the evaluation of the interfacial area, and not in the resistance definition, as a more rigorous derivation could show. However, we opted for this simple approach because most of the modelling uncertainties will anyway lie in this assumption and in the evaluation of dissolution rates.

It is evident that the present model formulation relies on simplifying assumptions that restrict its direct applicability to more complex real emulsions. These include the fact that the evolution of only one droplet is described, the fixed post-stimulus contact angle, the neglect of particle aggregation and multilayer adsorption, and the assumption that all particles have the same aspect ratio. The present model formulation is best interpreted as a local description of how interfacial particle dissolution affects surface coverage and, in turn, active ingredient diffusion, rather than as a complete representation of all phenomena that may occur in real concentrated emulsions. These assumptions were deliberately adopted to isolate this coupling in a tractable first modeling framework.

Nevertheless, our presented framework can also be extended, in principle, to more complex situations than those considered here. For example, a droplet size distribution could be incorporated by coupling the present formulation with an additional population balance over droplet size, although this would significantly increase the dimensionality of the problem and its computational cost. If droplet curvature becomes important, the geometrical relation used to evaluate covered and exposed particle area would need to be modified through more detailed geometrical corrections. Likewise, if crystal packing and preferred orientation at the interface become significant, the effective covering fraction could be refined by introducing corrections accounting for particle arrangement and packing constraints. This is consistent with our recent work on random sequential adsorption of Pickering particles onto spherical droplet surfaces (Feng et al., 2025), where curvature, finite-size, and local arrangement effects were treated explicitly. Finally, the present population balance framework can accommodate size-dependent dissolution kinetics directly, by replacing the current size-independent dissolution expression with a more detailed constitutive law. In practice, however, such laws are often not available in sufficient experimental detail, whereas simplified empirically fitted expressions are more commonly used. These extensions are beyond the scope of the present work, but they remain compatible with the overall modelling approach proposed here.

Regarding the mass transfer coefficients k_d and k_c, we evaluated them considering an immobile spherical drop in a stagnant continuous phase, considering the Sherwood number (Sh) equal to 2. Therefore, using the definition of Sherwood number, it is possible to evaluate them

as follows:

$$k_d = \frac{Sh\mathscr{D}_d}{d_d} \tag{13}$$

$$k_c = \frac{Sh\mathscr{D}_c}{d_d} \tag{14}$$

where $\mathscr{D}_d$ and $\mathscr{D}_c$ are the diffusivity of the AI in the droplet and in the continuous phase, respectively.

3. Numerical details

The model to be solved is constituted by the numerical solution of Eq. (2), (6), (10) and (11). In the literature many approaches are available to solve Eq (2) (Kumar et al., 2014; Marchisio and Fox, 2005; Marchisio et al., 2003; Gunawan et al., 2004; Doraiswami, 2000; Pigou et al., 2018; Leveque and Methods, 2002; Szilágyi and Nagy, 2016). Here we decided to opt for the most effective one for dissolution problems, the High-Resolution Finite Volume method (HRFVM) (Gunawan et al., 2004; Leveque and Methods, 2002), since Eq. (2) is a hyperbolic equation. A high-resolution discretization scheme for the convective equation (the second left hand side term of Eq. (2)) is needed to avoid unphysical oscillations in the solution or negative values for the number of particles. Details of the numerical discretization and of the internal coordinate space (i.e., particle size L) and temporal convergence analysis are reported in the Supporting Information. Based on this analysis, the numerical resolution adopted in the simulations for the internal coordinate space is a uniform grid with 500 intervals. The time integration of Eq. (16) is carried out using the Numerical Differencing Formula (NDF) scheme (i.e., Matlab ode15s), together with the solution of the other ordinary differential equations of the model (i.e., Eqs. (6), (10) and (11)). The solution algorithm is implemented in Matlab 2024 (Shampine et al., 1997; Shampine et al., 1999).

The initial particle size distribution (PSD) of the Pickering crystals is assumed having a lognormal shape in all the simulations performed, namely:

$$f_n(L) = \frac{\exp\left(-\frac{(\ln L-\mu)^2}{2\sigma^2}\right)}{L\sigma\sqrt{2\pi}} L > 0 \tag{15}$$

where $f_n(L)$ is the probability distribution of a lognormal function, which in our case indicates the numeric density of the particles of dimensions between L and $L + dL$.

The lognormal parameters μ and σ are directly linked to the mean m and variance v of the crystal size distribution represented by the adopted lognormal function, through Eqs. (16) and (17):

$$\mu = \log\left(\frac{m^2}{\sqrt{v+m^2}}\right) \tag{16}$$

$$\sigma = \sqrt{\log\left(\frac{v}{m^2+1}\right)} \tag{17}$$

In the case of lognormal distributions these two parameters are easier to work with respect to the classic mean and variance since they are easier to interpret (Limpert et al., 2001). The modeling choice made for the shape of the particle size distribution aligns with the experimental findings of Del Duca et al. (Del Duca et al., 2024); nevertheless, the model itself does not have any limitation on the initial particle size distribution that could be considered.

In order to better link the distribution parameters with measurable properties of the Pickering particles, in the following sections the mean m and variance v will be referred to, respectively, as *Crystal Average Size* (*CAS*) and *Standard Deviation* (*SD*). The expression *Mean Aspect Ratio (MAR)* will be instead used to identify the average value of the aspect ratio ϕ in the particles distribution.

Table 1 reports all the physical constants adopted in this work and the numerical values selected for the simulations. The values reported in Table 1 were selected to define a representative and physically plausible single-droplet release scenario for model illustration and parametric analysis. They were not intended to reproduce a specific dissolution method or any other standardized experimental protocol. In particular, the continuous-phase volume V_c should be interpreted here as a model parameter describing the surrounding medium available for dilution and transport around the droplet after administration or dilution, rather than as the volume of a specific dissolution apparatus.

Table 1
System default variables, used as starting point to then define the simulations.

	Solid particles Data		
Variable	Symbol	Unit	Value
Crystal Average Size (CAS)	m	m	10e-6
Standard Deviation (SD)	sd	m	2.5e-6
Molar Mass (Mw)	M_w	kg/mol	0.3684
Mass of particles	m_p	kg	1.5e-9
Density of particles	ρ	kg/m^3	1293
Aspect Ratio	Φ	–	–
Mean Aspect Ratio (MAR)	–	–	3.5
Particles Solubility	C_{solub}	mol/m^3	0.01
Growth constant	k_g	m/s	5e-9
	Active Ingredient Data		
Diffusion Coefficient in dispersed phase	D_{p1}	m^2/s	1e-9
Diffusion Coefficient in continuous phase	D_{p2}	m^2/s	1e-10
Partition Coefficient	P	–	0.5
	System Data		
Droplet diameter	d	m	0.5e-3
Radius of continuous phase sphere	R	m	6e-3
Initial concentration of solute in dispersed phase	$C_{0,AI,d}$	mol/m^3	700
Initial concentration of solute in continuous phase	$C_{0,AI,c}$	mol/m^3	0

Table 2 shows a summary of all the simulations performed by varying different properties related to the Pickering particles, such as the *CAS* and *SD* of the *PSD*, the *Mean Aspect Ratio*, *MAR*, and the dissolution rate of the Pickering particles. We explore also the effect of the solubility of Pickering particles in the continuous phase, the affinity of the AI to different phases and the volume of the continuous phase (i.e., dilution effect upon administration). The design rationale for these simulations was driven by the need to understand how the properties of Pickering particles affect the release of AI. As a control case, the release of AI from a standard emulsion, without Pickering particles, was estimated (e.g., covering fraction equal to zero, only AI diffusion as physical

Table 2
Simulations design.

Simulation No.	Simulation name	Variable changed	Values
1	Sim_CAS_1	CAS	5×10^{-6}
2	Sim_CAS_2		10×10^{-6}
3	Sim_CAS_3		15×10^{-6}
4	Sim_SD_1	SD	1×10^{-6}
5	Sim_SD_2		2.5×10^{-6}
6	Sim_SD_3		5×10^{-6}
7	Sim_AR_1	MAR	1
8	Sim_AR_2		3.5
9	Sim_AR_3		5
10	Sim_kg_1	Mass Transfer	5×10^{-8}
11	Sim_kg_2	Coefficient	5×10^{-9}
12	Sim_kg_3		5×10^{-10}
13	Sim_solub_1	Particles Solubility	0.005
14	Sim_solub_2		0.01
15	Sim_solub_3		1
16	Sim_P_1	Partition	0.5
17	Sim_P_2	Coefficient	0.067
18	Sim_P_3		0.01

phenomenon).

4. Results & Discussion

4.1. Simulations results

After verification of the optimal numerical discretization (see Supporting Information), the model was used to analyze how Pickering particle population properties affect interfacial coverage evolution and active ingredient release. As mentioned in Section 3, we performed different simulations by varying different parameters related to the emulsion formulation, with the aim of building an intuitive explanation of the effect of Pickering particles properties on the release performance.

4.1.1. Initial covering fraction

The covering fraction f is a key parameter that affects the rate of AI release at it determines the area available for mass transfer between the disperse and continuous phase. The covering fraction depends on the amount, size and shape distributions of the Pickering particles surrounding the droplet. Hence, in this section we investigate how Pickering particles properties affect the value of f. As we assumed a monolayer of crystals with only one face in contact with the interface, we kept f below 0.95. This constraint arises from the inherent limitation in particle packing caused by our assumptions, where the achievable coverage is restricted by particle hindrance and their varying orientations. The study of the initial coverage fractions in the various simulations was conducted by maintaining all model parameters from Table 1 constant, except for the one whose influence was investigated. The variables tested were the *Crystal Average Size (CAS)*, the *Standard Deviation (SD)*, the initial total mass of Pickering particles and the *Mean Aspect Ratio (MAR)*. Fig. 2-a shows how the CAS affects the coverage of the droplet. A non-monotonic behavior is observed, with an initial increase up to a maximum at 2 μm, followed by a decrease and then a plateau at larger CAS values. This behavior arises because, in these simulations, the total crystal mass is kept constant. At low CAS values, the number of crystals is high and their surface-to-volume ratio is favorable for interfacial coverage. However, each individual crystal covers only a very small interfacial area. As the CAS increases from very small values, the area covered by each crystal increases while the number of crystals is still sufficiently high, leading to an increase in the overall covering fraction. The maximum at 2 μm corresponds to the most favorable balance between the number of crystals and the interfacial area covered by each crystal. With further increase in the CAS, the reduction in crystal number becomes dominant, and the covering fraction decreases.

The effect of the *SD* of the Pickering PSD on the covering fraction was also investigated. This value can be seen as a measure of initial polydispersity of the PSD. In Fig. 2-b it is possible to see a decreasing trend for the covering fraction as the *SD* increases, for fixed values of mass, *CAS* and *MAR* of the Pickering particles. The coverage decreases, although less compared to the trend observed for the *CAS*, by increasing PSD polydispersity. This is due to the lognormal nature of the PSD, which has a bigger tail at the right end compared to the left; hence, increasing *SD* determined a higher number of larger crystals, which results in lower covering fractions.

In Fig. 2-c it is possible to observe how the total mass of Pickering crystals affects the covering fraction. As expected, increasing the number of crystals determined an increase in the covering fraction. By varying the *MAR* of the Pickering particles, as shown in Fig. 2-d, a similar trend can be observed. The *MAR* directly affects the droplet surface area occupied by the largest Pickering crystal faces. By increasing the *MAR* at constant *CAS*, the area of the droplet occupied by the largest Pickering crystal faces increases.

It should be remarked that none of these considerations consider the actual packing and orientation of crystals, which can affect the maximum coverage value.

4.1.2. Evolution of the PSD upon dissolution

Fig. 3 shows a simulated evolution in time of the PSD of the Pickering particles due to their dissolution. As previously mentioned, the use of Eq. (5) for $G(L,t)$ leads to an equal dissolution rate for all the particles, meaning that the distribution shifts to the left with an equal velocity for all the particles, and with a speed that decreases over time due to the change of undersaturation (as seen in Eq. (6)). Fig. 3 demonstrates the capability of the HRFV method to solve a dissolution problem, since solution is limited between the initial maximum value and zero, and the unavoidable numerical diffusion does not produce significant artifacts on the numerical solution, with the maximum value that is equal to 0.99 times the maximum value when the left boundary is crossed. Eventually, the final state reported in the Figure corresponds to full dissolution of all Pickering particles, showing that the numerical method is able to properly describe also this particular case.

4.1.3. Effect of PSD on the AI release

In this subsection, we examine the influence of how different Pickering PSDs affect the rate of AI release. To systematically assess this effect, we adopted the methodology outlined in Section 3, wherein a single property is altered at a time while maintaining all other variables constant, as already presented in Table 2. Fig. 4 illustrates the outcomes when only the *CAS* is modified.

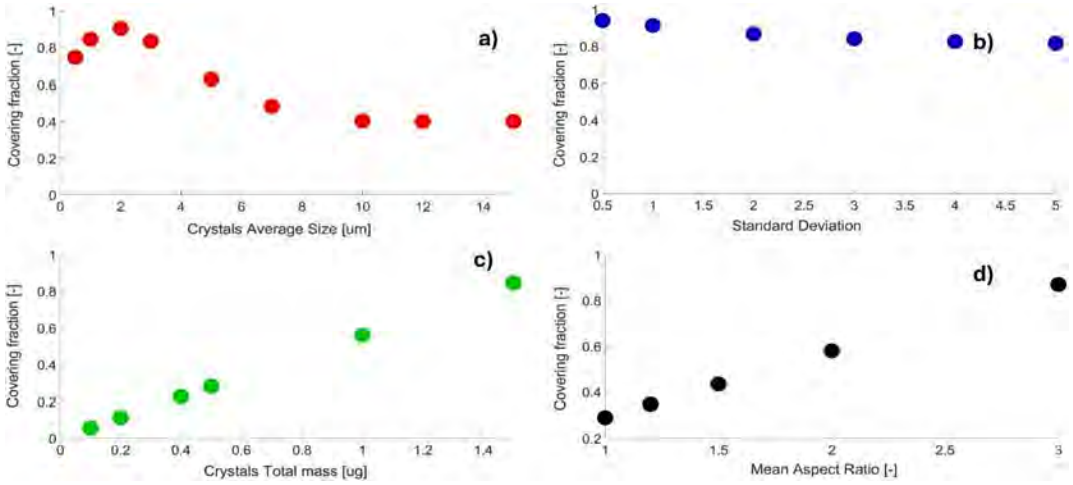

Fig. 2. Influence of crystals population variables on the initial covering fraction. a) Influence of Crystal Average Size b) Influence of Standard Deviation c) Influence of Crystal Mass d) Influence of Mean Aspect Ratio.

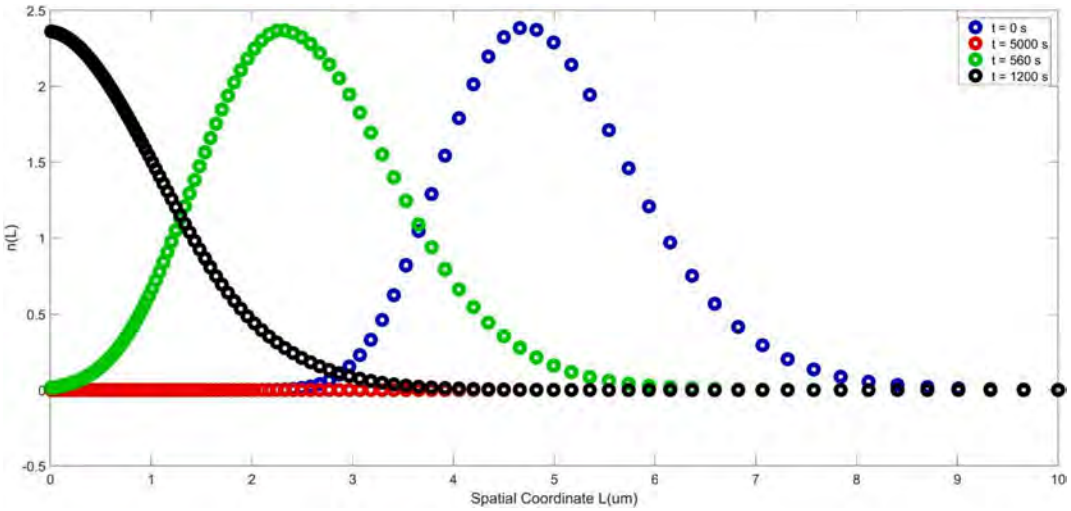

Fig. 3. Distribution evolution over time during dissolution.

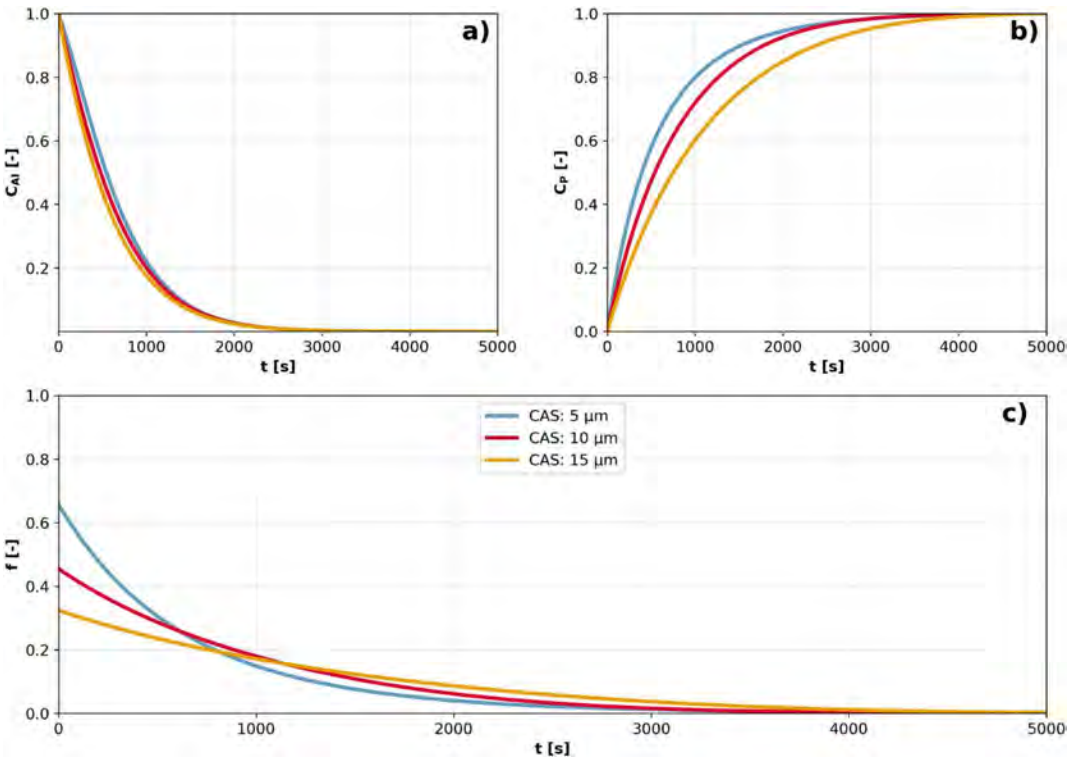

Fig. 4. Model prediction for different CAS values: a) AI Concentration in the dispersed phase over time b) Pickering crystal solute concentration over time in the continuous phase c) Covering fraction over time.

The model predicts the temporal evolution of the AI concentration (C_{AI}), the concentration of the Pickering particles dissolved in the continuous phase (C_P) and the covering fraction (f) for three different values of the *CAS*. As shown in Fig. 2 increasing the *CAS* beyond 2 μm results in a reduced initial covering fraction (Fig. 4-c), which in turn accelerates the onset and enhances the rate of AI release (Fig. 4-a). On the other hand, C_P increases at a slower rate for larger particles, due to their lower surface to volume ratio (Fig. 4-b). Hence, the reduction in initial f value due to higher *CAS* prevails over the slower Pickering particles dissolution, enhancing the release rate of AI, especially in the first 700 s (Fig. 4-a). At longer times (> 1000s) the slower Pickering particles dissolution balances the initially higher covering fraction, resulting in identical profiles for the C_{AI}.

The *CAS* is not the only parameter of the initial PSD of Pickering particles that can be manipulated to modify the AI release. In fact, it is also possible to modify the polydispersity (*SD*) of the PSD. A PSD with high polydispersity is characterized by crystals with a wider variety of sizes, affecting significantly the initial value of the covering fraction as shown in Section 3 and Fig. 5-c.

Fig. 5 shows simulations obtained varying the *SD* of the Pickering PSD. As observed in Fig. 2, higher *SD* values generate lower covering fractions. On the other hand, the dissolution rate of Pickering particles (Fig. 5-b) is slower for higher SD values. Hence, increasing *SD* generates the same trend of the *CAS*, both in the concentration of AI and in the evolution of the covering fraction. From Fig. 5-b it can be seen clearly that the more the Pickering particles are polydisperse, the higher their

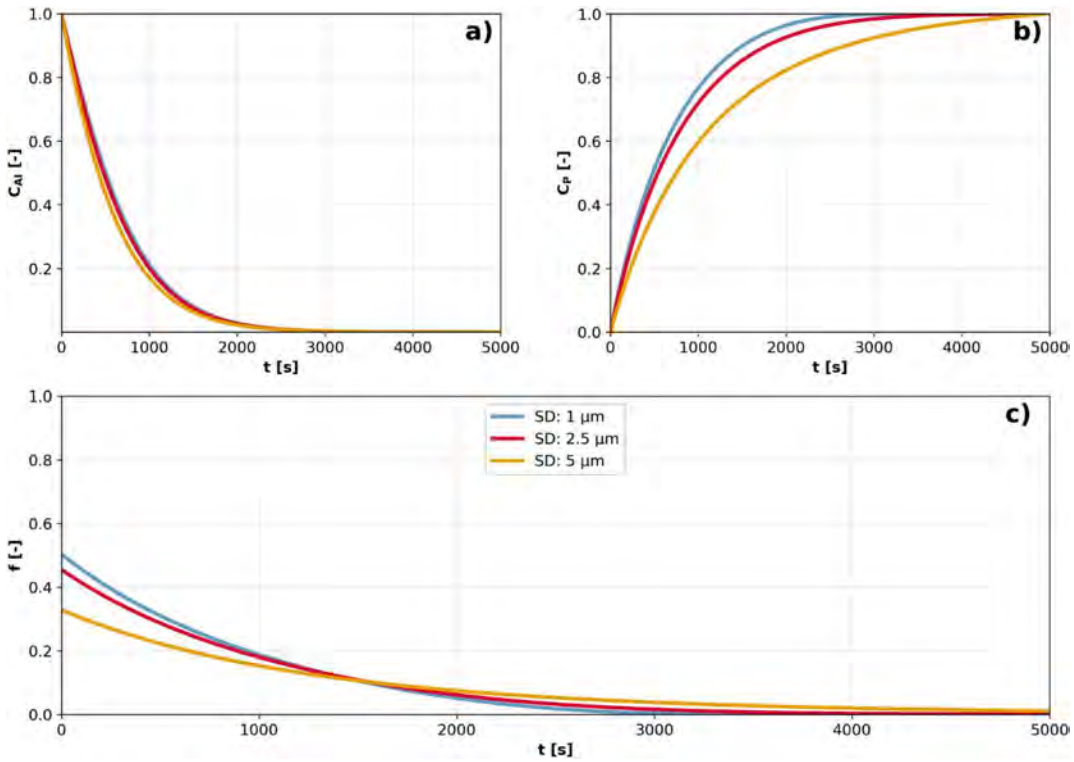

Fig. 5. Model prediction for different SD values: a) AI Concentration in the dispersed phase over time b) Crystal compound concentration over time in the continuous phase c) Covering fraction over time.

dissolution time, since larger particles requires more time to dissolve, at equal total Pickering particles mass and volume.

Lastly the *Mean Aspect Ratio (MAR)* of the Pickering PSD was varied to see how crystals with different shapes could change the rate of AI release.

As shown in Fig. 6-a cubic crystals ($MAR = 1$) determine the quicker release since they correspond to the lower initial covering fraction, as opposed to needle-like crystals that tend to be more efficient in slowing

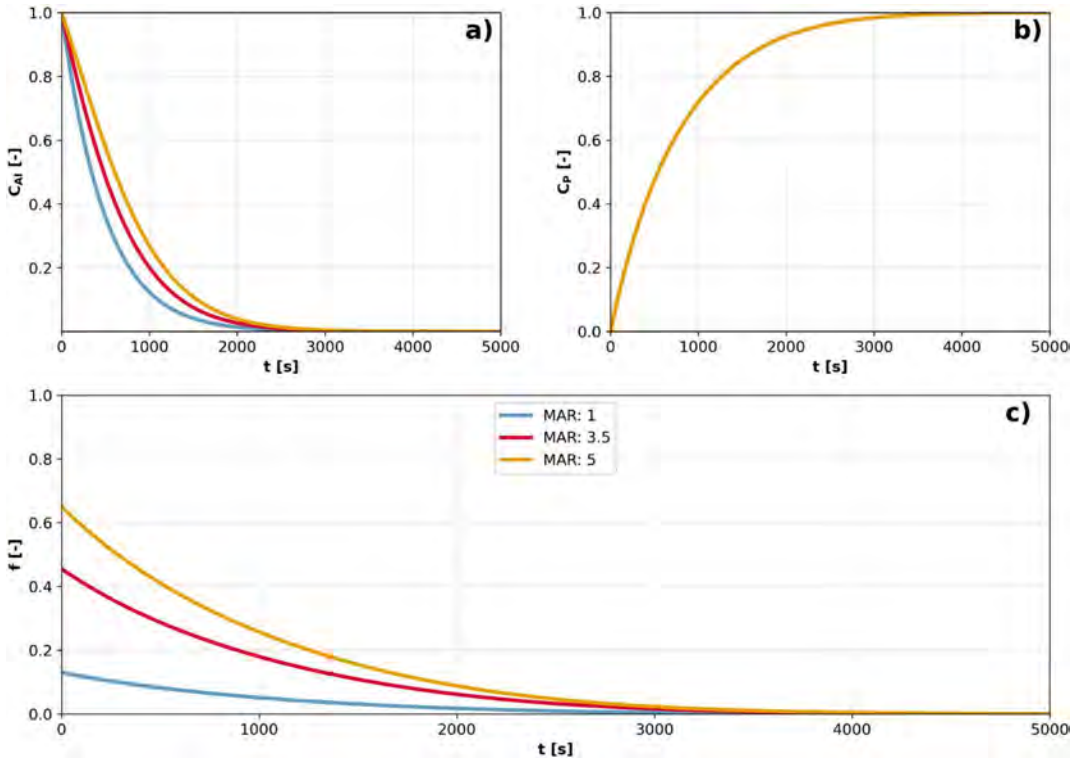

Fig. 6. Model prediction for different Mean Aspect Ratio values: a) AI Concentration in the dispersed phase over time b) Crystal compound concentration over time in the continuous phase c) Covering fraction over time.

down the release of the AI. At the same time, in Fig. 6-b it is possible to observe that the aspect ratio of the Pickering crystals does not affect their dissolution rate in the chosen range between 1 and 5. This is expected since dissolution rate (Eq. (5)) is not a function of the particle size and/or aspect ratio. It is worth noting that, considering the assumption made in our simulations, values of $MAR>5$ would determine only a partial wetting of the largest face of Pickering particles, due to the curvature of the droplet surface. In such case, the model assumption of one face fully adsorbed at the interface would not hold anymore. The weak effect of *MAR* variation on the dissolution can be attributed to the way the model is built: the PSD shape in fact is mainly affected by the *Crystal Average Size* and by the *Standard Deviation*, since they appear directly into Eqs. (15) to (17). The *MAR* instead does not directly define the shape of the PSD, but simply changes the number of particles that we have in the system, by the volume factor $\frac{1}{\phi^2}$, as the mass remains constant but the volume decreases for particles with higher *Mean Aspect Ratio*. This exaplains why the the crystal compound concentration evolution over time is the same in the simulations of all the three different MARs.

These results for the *Mean Aspect Ratio* seem to follow a similar trend to the one observed experimentally (Madivala et al., 2009; Lou et al., 2016), where to obtain good stability for Pickering emulsions it was necessary to have a minimum value of *MAR* for the particles. Madivala et al. (Madivala et al., 2009) also suggested a possible correlation between MAR and the covering fraction itself.

Fig. 7 illustrates effect of Pickering particles with different *CAS, MAR* and *SD* on the rate of AI release. In particular, the figure show the times necessary to reach 70% of release of AI from the droplet. It is evident that Pickering particles can slow down the release, and further modulation can be achieved by manipulation of the PSD properties. In some conditions the release time can improve the release of up to 1.6 times compared to the control conditions (i.e., emulsion without Pickering particles).

The results of this section are in agreement with experimental observations, as summarized in Table 3. A precise quantitative validation of the present model against literature data is not currently possible, because published studies generally do not provide the complete and internally consistent set of measurements required for this purpose. For this reason, the literature comparison presented here is limited to qualitative trend consistency. It was previously observed that smaller *CAS* can provide better stabilization, with high f values and slower release rate (Binks and Lumsdon, 2001; Qi et al., 2014; Aslan Türker and Işçimen, 2025). Also, the effect of different *MAR* values for the Pickering crystals seem to follow the correct experimental trends, as crystals with higher aspect ratio showed the same effect as the crystals with larger size, decelerating the release and increasing the coverage of the droplet (Madivala et al., 2009; Kalashnikova et al., 2011).

4.1.4. Effect of Pickering crystal compound on the release of AI

Another important choice that could impact the AI release rate is the type of Pickering crystals used for stabilization. The solubility and dissolution kinetics in the continuous phase of Pickering particles can be modified by using different polymorphs of the same chemical species, or by changing altogether the chemical species characterizing the Pickering particles. It is worth noticing that this change would also affect the contact angle; however, in our simulations we considered the same value for simplicity.

It is evident that the choice of the type of crystalline Pickering particles can be a further strategy to modulate the release of AI.

In order to simulate the effect of different particles we modified the kg parameter (Eq. (5) of the dissolution kinetic expression (Fig. 8) and the solubility of the Pickering crystals (Fig. 9).

By decreasing k_g the dissolution of Pickering particles is slower, causing a significant delay in the release of the AI (Fig. 8-a). This delay is due to slower decrease in covering fraction (Fig. 8-c), which is in turn related to the slower increase in concentration of the Pickering particles dissolved (Fig. 8-b).

Fig. 9 shows the effect of changing the solubility of the Pickering particles on the release rate of AI. As undersaturation is the driving force for dissolution, compounds with higher solubility in the continuous phase will dissolve faster, generating a faster decrease in the covering fraction and, hence, faster AI release.

As shown in Fig. 10 the change in polymorphic form or chemical species of the Pickering particles can strongly influence the rate of release of AI, particularly by modification of the k_g parameter. The order of magnitude of the release times and the trends obtained from the model simulations where the mass transfer coefficient was changed are plausible, and in agreement with previous literature, as also shown in Table 3 (Tang et al., 2019; Wood et al., 2018). In fact, higher solubility of the Pickering crystals, caused by an increase in temperature determined a faster AI release rate in the study of Li et al. (n.d.) a similar effect was obtained when changing pH (Lan et al., 2007; Low et al., 2018).

4.1.5. Effect of type of active ingredient on its release rate

Although from the formulation perspective the objective of the work is usually to target the release of a specific AI, the model can be also used to screen between different AIs. To simulate this we modified the partition coefficient P in Eq.s (10) and (11). The partition coefficient of substances that are slightly hydrophobic is usually around 2 – 5, while a higher hydrophobic substance would present partition coefficients in the order of 100; whereas, more hydrophilic AIs would have values lower than 1. Pharmaceutical or agrochemical compounds are normally hydrophobic and are encapsulated in oil in water emulsions; we decided to simulate such case and choose values of $P>1$.

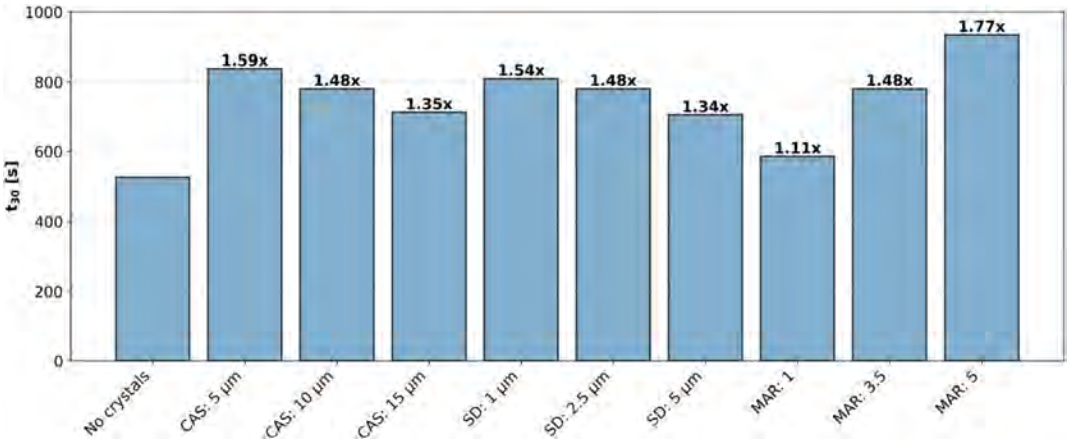

Fig. 7. Times for the release of 70% of AI encapsulated inside the droplet. The case with no Pickering crystals was considered as the control, the numbers for each other column has been obtained by dividing the calculate release times by the control one.

Table 3
Summary of experimental evidence for the proposed Pickering dissolution driven AI release.

Type of emulsion	Particles used	Type of experiment	Results	Model Confirmation	Reference
Oil (Decane) in Water/Water in Oil (Decane)	Hydrophobic prolate ellipsoids/Hydrophilic hematite particles	Emulsion stability test	Stable emulsions only obtained with particles with a sufficiently high aspect ratio	Higher MAR values determined increased emulsion stabilization, linked to higher covering fraction	(Pigou et al., 2018)
Oil (Hexadecane) in Water	Silica microrods	Emulsion stability test	Emulsions obtained with particles with higher Aspect Ratio are stable for longer	Particles with higher MAR are shown to deliver more stable emulsions due to higher covering fraction	(Leveque and Methods, 2002)
Oil (Ethyl Acetate) in Water	Poly(D,Llacticcoglycolicacid) particles	Emulsion stability test	Amongst the different parameters studied it was shown that a reduced particles size could improve the emulsions stability	Smaller particles showed a better tendency to stabilize emulsions due to higher covering fractions	(Xia et al., 2021)
Oil in Water	Hydrophobic and Hydrophilic Latex particles	Emulsion stability test	Larger particles produced larger droplets, following an increase in the sedimentation rate up to a certain size	The increase of the droplet sedimentation rate and the larger size of droplets observed for larger particles can signal a decrease in stability due to lower covering fraction	(Szilágyi and Nagy, 2016)
Oil (Hexadecane) in Water	Bacterial cellulose nanocrystals	Emulsion stability test	Elongated shape cellulose nanocrystals were able to stabilize oil in water emulsion for months	High MAR values generated more stable emulsions due to higher covering fraction	(Shampine et al., 1999)
MCT oil in Water	Phosphatidylcholine-kaolinite particles	Active Ingredient release test	The simulation of gastric and intestinal digestion environment showed different release times and trends as a function of different particle properties	The results showed how particle properties can modulate the release of encapsulated AIs	(Limpert et al., 2001)
Water in Canola Oil	Glycerol Monostearate crystals	Active Ingredient Release	Different release profiles observed for different encapsulated AIs, different interfacial stabilizers and their concentrations, and different temperatures	The results show a release rate dependence on: (i) the type of AI (e.g., different solubility, partition coefficient), (ii) temperature, which affects solubility, (iii) type and concentration of stabilizer	(Binks and Lumsdon, 2001)
Oil (soybean/corn/ hexane) in Water	Cellulose nanocrystals	Active Ingredient Release	Release profiles with strong temperature dependence	These results confirm the effect of increased temperature on the AI release: higher solubility and mass transfer coefficient determines faster release.	Li et al. (n.d.)
Oil (Paraffin) in Water	Bilayer oleic acid-coated Fe3O4 nanoparticles	Emulsion stability	Partition of the nanoparticles is affected by pH and ion strength and accordingly Pickering emulsions are also sensitive to pH and ion strength	The paper confirms that by changing the pH it is possible to affect the emulsion stability and release behavior	(Lan et al., 2007)

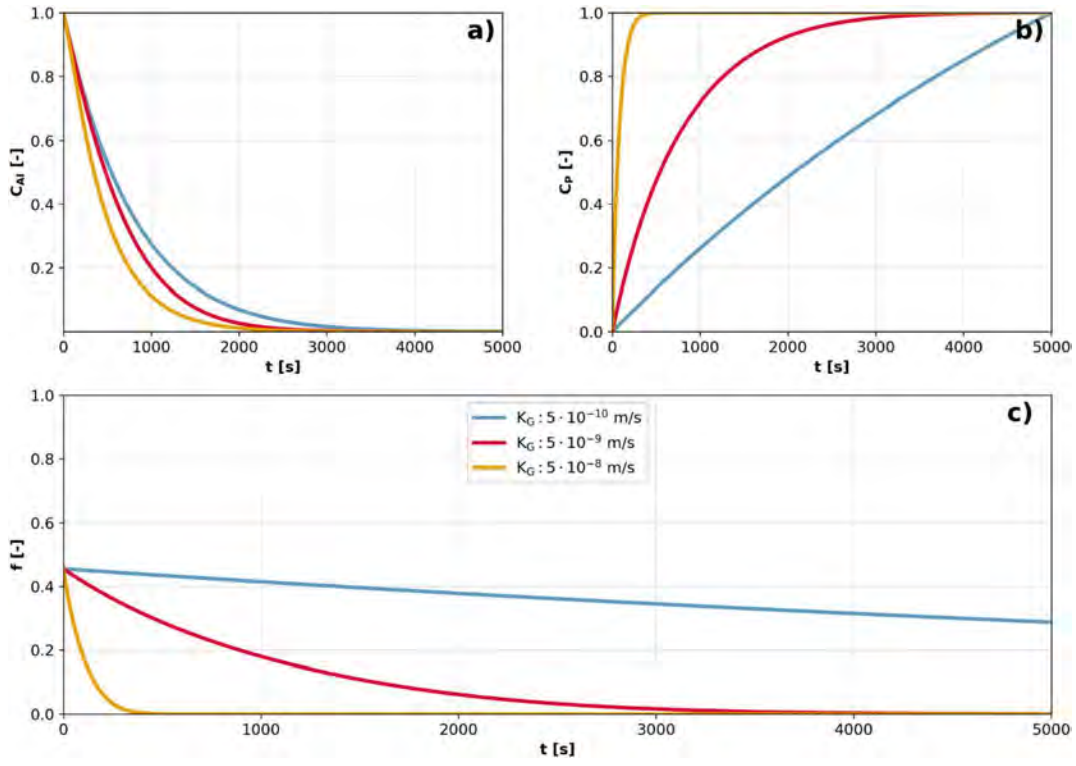

Fig. 8. Model prediction for different Kg values of: a) AI concentration in the dispersed phase over time b) Crystal compound concentration over time in the continuous phase c) Covering fraction over time.

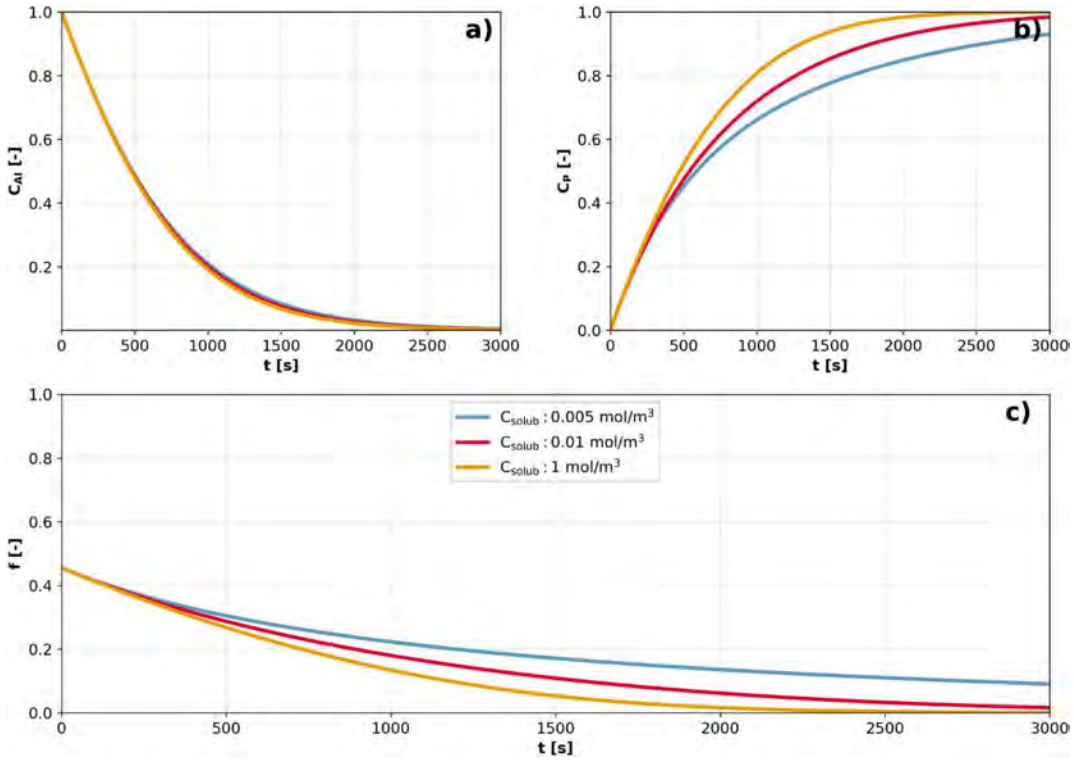

Fig. 9. Model prediction for different solubility values of: a) AI concentration in the dispersed phase over time b) Crystal compound concentration over time in the continuous phase c) Covering fraction over time.

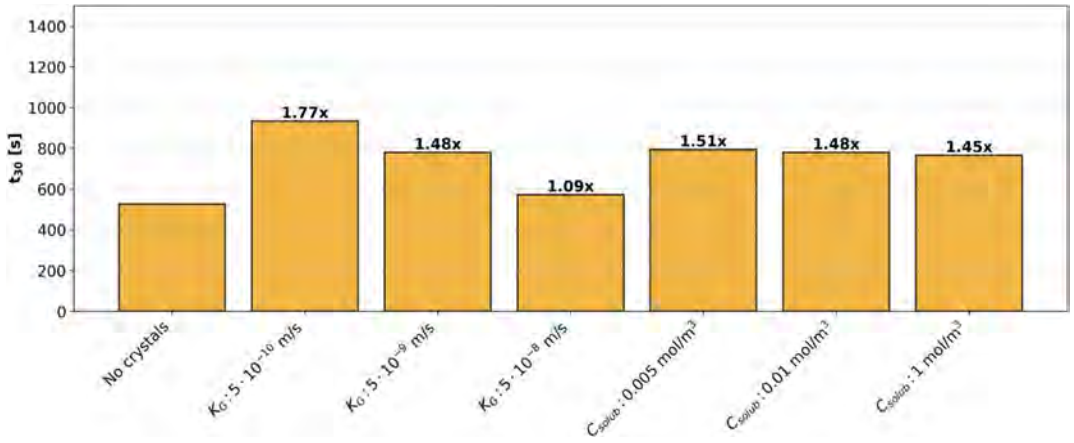

Fig. 10. Times for the Active Ingredient inside the droplet to reach 30% of the initial concentration in different simulations involving the crystal compound variation. Each column has the multiplier calculated with respect to the simulation with "no crystals".

Fig. 11 shows the results of the simulations for three values of *P* ranging from 2 to 109. It is clear that the partition coefficient has a strong effect on the release rate of AI; this has to be taken into consideration when designing Pickering particles. In fact, for high partition coefficients, with AI diffusing very slowly into the continuous phase, it is necessary to select Pickering particles with slower dissolution rate in order to enable effective modulation of the release rate. Indeed, for extremely high values of partition coefficient the presence of Pickering particles might not have any effect on the release rate (although they would still act as encapsulation agents to protect the AI from degradation).

Taken together, the results suggest a qualitative ranking of the relative impact of the explored variables on AI release, within the ranges considered in this work. The strongest effects are associated with the partition coefficient of the AI and with the dissolution behavior of the Pickering particles, especially the dissolution kinetic parameter and particle solubility, since they directly affect the release driving force and the rate at which the interfacial barrier is removed. By contrast, particle population properties such as crystal average size, aspect ratio, and size distribution influence release mainly through their effect on the initial covering fraction and its subsequent evolution. From a formulation perspective, it is also useful to distinguish between system-dependent parameters and formulation-adjustable ones. While the partition coefficient of the AI and, to a large extent, the dissolution behavior of the Pickering particles depend on the selected chemical system, the main practical route to slow down or fine-tune release, once the system has been fixed, is to act on the Pickering layer itself, for example through changes in particle size and shape distributions, as well as particle loading. These variables determine the initial interfacial coverage and its evolution during dissolution.

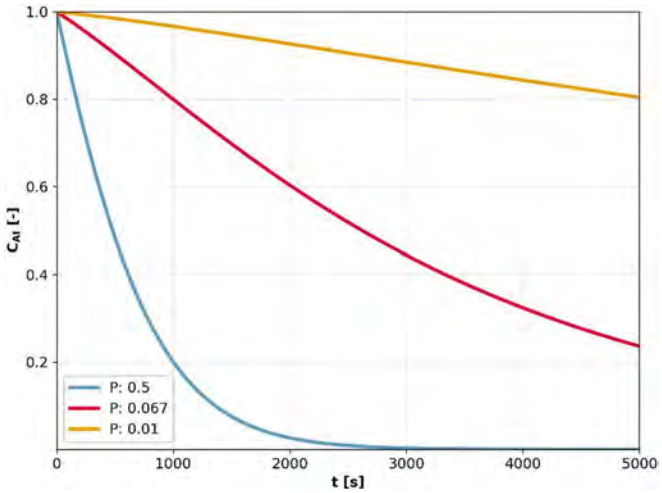

Fig. 11. AI concentration in the dispersed phase over time at different values of the Partition Coefficient.

In conclusion, the results obtained from the presented simulations show a clear and strong influence of the properties of Pickering crystals on the rate of AI release from a Pickering emulsion. This opens up possibilities for crystal engineers to design optimized Pickering particles to enable finely controlled AI release.

5. Conclusions

A PBE-based model was developed to describe the release of an AI from the dispersed phase of a Pickering emulsion. The model considered a single droplet of dispersed phase, immobilized within a larger volume of continuous phase. Equations were implemented in order to simultaneously describe both the temporal evolution of the Pickering PSD, as particles dissolve upon administration, and the release of the AI encapsulated in the droplet. The dispersed and continuous phases, defined by using different diffusion coefficients for the AI, were oil as the dispersed phase and water as the continuous one (oil in water emulsion). The Pickering crystals were considered as rectangular rods in contact with the droplet surface only with one of their six faces, and only their dissolution was considered in the PBE. The mass transfer for the AI was modeled using a mass balance at the interface and Fick's law. The ability of the model to correctly and realistically describe the AI release from a Pickering emulsion was tested by varying Pickering particles properties and simulating the AI concentration in the continuous phase over time. The simulations results show trends aligned with what reported in experimental studies previously published: smaller and elongated crystals slow down the release of AI as they more efficiently cover the droplet surface reducing the area available for diffusion. At the same time, the variation of the mass transfer coefficient k_g and the Pickering particles solubility, which can be achieved by changing the crystal structure of the chemical species of the Pickering particles, was found to have a strong effect on the AI release rate. Changes in these two parameters could also be determined by a change in pH or temperature, demonstrating the possibility of using the model for the design of stimuli-responsive Pickering formulations.

The present model focuses on the effect of Pickering particle dissolution through the evolution of interfacial coverage and the corresponding area available for active ingredient mass transfer. In real systems, however, additional mechanisms may also play a role. For example, dissolution of the Pickering particles may modify the local physicochemical environment at the interface, including pH, solute composition, and possible interactions with the active ingredient, thereby affecting solubility or partitioning. In other systems, the formation of interfacial or gel-like layers may introduce an additional resistance to mass transfer. These effects are beyond the scope of the present formulation, but they represent important directions for future extensions of the model.

Overall, this work presents a framework that can assist formulators in screening formulation strategies and in interpreting how Pickering particle population properties affect active ingredient release. Quantitative optimization for specific systems would require dedicated experimental calibration and validation.

CRediT authorship contribution statement

Pierfrancesco Latorre: Writing – original draft, Investigation, Formal analysis, Data curation. **Antonio Buffo:** Writing – review & editing, Supervision, Methodology, Investigation, Formal analysis, Data curation, Conceptualization. **Elena Simone:** Writing – review & editing, Validation, Supervision, Resources, Project administration, Methodology, Formal analysis, Conceptualization.

Declaration of competing interest

The authors declare that they have no known competing financial interests or personal relationships that could have appeared to influence the work reported in this paper.

Acknowledgments

This project has received funding from the European Research Council (ERC) under the European Union's Horizon 2020 research and innovation program (grant agreement No. 949229, CryForm). The authors wish to express their appreciation to Giulia Del Duca for her assistance and the useful discussions on crystals stabilized Pickering emulsions and their stability.

Appendix A. Supplementary data

Supplementary data to this article can be found online at https://doi.org/10.1016/j.ces.2026.124620. The supporting information document present: (1) description of the size discretization method; (2) numerical error analysis, (3) a modification of the model to represent the effect of lipase on particle dissolution.

Data availability

All codes used in this work are available at https://doi.org/10.5281/zenodo.21283980.

References

S.K. Abdul Mudalip, M.R. Abu Bakar, P. Jamal, F. Adam, R. Che Man, S.Z. Sulaiman, Z.I. Mohd Arshad, S. Md Shaarani, Effects of Solvents on Polymorphism and Shape of Mefenamic Acid Crystals, in: MATEC Web of Conferences, EDP Sciences, 2018. https://doi.org/10.1051/matecconf/201815002004.

Aslan Türker, D., Işçimen, E.M., 2025. Insoluble dietary fiber and microparticle formation from olive pomace: effects on emulsification and interfacial behavior in Pickering emulsions. J. Food Meas. Charact. https://doi.org/10.1007/s11694-025-03139-3.

R. Aveyard, B.P. Binks, J.H. Clint, Emulsions stabilised solely by colloidal particles, 2003.

Barlow, D.A., LaVoie-Ingram, E., Bayat, J., 2022. Population-balance study of protein crystal growth from solution using a hyperbolic rate law. J. Cryst. Growth 578. https://doi.org/10.1016/j.jcrysgro.2021.126417.

Binks, B.P., Lumsdon, S.O., 2000. Influence of particle wettability on the type and stability of surfactant-free emulsions. Langmuir 16, 8622–8631. https://doi.org/10.1021/la000189s.

Binks, B.P., Lumsdon, S.O., 2001. Pickering emulsions stabilized by monodisperse latex particles: Effects of particle size. Langmuir 17, 4540–4547. https://doi.org/10.1021/la0103822.

R.B. Bird, W.E. Stewart, E.N. Lightfoot, Transport Phenomena, 2002.

Bosetti, L., Mazzotti, M., 2020. Population balance modeling of growth and secondary nucleation by attrition and ripening. Cryst. Growth Des. 20, 307–319. https://doi.org/10.1021/acs.cgd.9b01240.

Briese, L., Arvidson, R.S., Luttge, A., 2017. The effect of crystal size variation on the rate of dissolution – A kinetic Monte Carlo study. Geochim. Cosmochim. Acta 212, 167–175. https://doi.org/10.1016/j.gca.2017.06.010.
Brunier, B., 2015. Modeling of Pickering Emulsion Polymerization. Université Claude Bernard-Lyon I). Doctoral dissertation.
Brunier, B., Chevalier, Y., Bourgeat-Lami, E., Sheibat-Othman, N., 2022. Modeling polystyrene homogeneous-coagulative nucleation in pickering emulsion polymerization. Macromol. React. Eng. 16 (6), 2200016.
Chaudhury, A., Kapadia, A., Prakash, A.V., Barrasso, D., Ramachandran, R., 2013. An extended cell-average technique for a multi-dimensional population balance of granulation describing aggregation and breakage. Adv. Powder Technol. 24, 962–971. https://doi.org/10.1016/j.apt.2013.01.006.
Chen, L., Ao, F., Ge, X., Shen, W., 2020. Food-grade pickering emulsions: preparation, stabilization and applications. Molecules 25. https://doi.org/10.3390/molecules25143202.
da Ferreira, G.S., da Silva, D.J., Zanata, L., Souza, A.G., Ferreira, R.R., Rosa, D.S., 2022. Antimicrobial cotton wipes functionalized with Melaleuca alternifolia Pickering emulsions stabilized with cellulose nanofibrils. Carbohydr. Polym. Technol. Appl. 3. https://doi.org/10.1016/j.carpta.2022.100208.
Dan, N., 2016. Transport and release in nano-carriers for food applications. J. Food Eng. 175, 136–144.
de Carvalho-Guimarães, F.B., Correa, K.L., de Souza, T.P., Rodríguez Amado, J.R., Ribeiro-Costa, R.M., Silva-Júnior, J.O.C., 2022. A review of pickering emulsions. Perspect. Appl. Pharmaceut. 15. https://doi.org/10.3390/ph15111413.
Del Duca, G., Parisi, E., Artusio, F., Calì, E., Fraterrigo Garofalo, S., Rosso, C., Cauda, V., Chierotti, M.R., Simone, E., 2024. A crystal engineering approach for rational design of curcumin crystals for Pickering stabilization of emulsions. Food Res. Int. 194, 114871. https://doi.org/10.1016/j.foodres.2024.114871.
Dighe, A.V., Nemade, R.Y., Singh, M.R., 2019. Modeling and simulation of crystallization of metal–organic frameworks. Processes 7. https://doi.org/10.3390/PR7080527.
Doraiswami. Ramkrishna, Population balances : theory and applications to particulate systems in engineering, Academic Press, 2000.
Y. Feng, G. Del Duca, A. Buffo, e E. Simone. Random sequential adsorption of Pickering particles onto spherical emulsion droplet surfaces, *Phys. Rev. E*, vol. 112, fasc. 6, p. 065506, dic. 2025, doi: 10.1103/hkc7-5dfm.
Frelichowska, J., Bolzinger, M.-A., Pelletier, J., Valour, J.-P., Chevalier, Y., 2009. Topical delivery of lipophilic drugs from o/w Pickering emulsions. Int. J. Pharm. 371, 56–63. https://doi.org/10.1016/j.ijpharm.2008.12.017.
Frungieri, G., Briesen, H., 2023. A population balance model for the flow-induced preparation of Pickering emulsions. Chem. Eng. Res. Des. 189, 694–706. https://doi.org/10.1016/j.cherd.2022.11.037.
Gagliardi, L., Pierre-Louis, O., 2018. Thin film modeling of crystal dissolution and growth in confinement. Phys. Rev. E 97. https://doi.org/10.1103/PhysRevE.97.012802.
Ghosh, S., Rousseau, D., 2011. Fat crystals and water-in-oil emulsion stability, Curr Opin Colloid. Interface Sci. 16, 421–431. https://doi.org/10.1016/j.cocis.2011.06.006.
D. Gonzalez Ortiz, C. Pochat-Bohatier, J. Cambedouzou, M. Bechelany, P. Miele, Current Trends in Pickering Emulsions: Particle Morphology and Applications, Engineering 6 (2020) 468–482. https://doi.org/10.1016/j.eng.2019.08.017.
Gunawan, R., Fusman, I., Braatz, R.D., 2004. High resolution algorithms for multidimensional population balance equations. AIChE J. 50, 2738–2749. https://doi.org/10.1002/aic.10228.
Hiranphinyophat, S., Otaka, A., Asaumi, Y., Fujii, S., Iwasaki, Y., 2021. Particle-stabilized oil-in-water emulsions as a platform for topical lipophilic drug delivery. Colloids Surf. B Biointerfaces 197. https://doi.org/10.1016/j.colsurfb.2020.111423.
Hu, X., Binks, B.P., Cui, Z., 2022. Water-in-oil Pickering emulsions stabilized by edible surfactant crystals formed in situ. Food Hydrocoll. 125. https://doi.org/10.1016/j.foodhyd.2021.107394.
Kalashnikova, I., Bizot, H., Cathala, B., Capron, I., 2011. New pickering emulsions stabilized by bacterial cellulose nanocrystals. Langmuir 27, 7471–7479. https://doi.org/10.1021/la200971f.
Klink, I.M., Phillips, R.J., Dungan, S.R., 2011. Effect of emulsion drop-size distribution upon coalescence in simple shear flow: a population balance study. J. Colloid Interface Sci. 353 (2), 467–475.
J. Kumar, M. Peglow, G. Warnecke, S. Heinrich, E. Tsotsas, L. Mörl, M. Hounslow, G. Reynolds, Numerical Methods on Population Balances, in: Modern Drying Technology, Wiley, 2014: pp. 209–260. https://doi.org/10.1002/9783527631728.ch6.
Lan, Q., Liu, C., Yang, F., Liu, S., Xu, J., Sun, D., 2007. Synthesis of bilayer oleic acid-coated Fe3O4 nanoparticles and their application in pH-responsive Pickering emulsions. J. Colloid Interface Sci. 310, 260–269. https://doi.org/10.1016/j.jcis.2007.01.081.
Lasaga, A.C., Lüttge, A., 2003. A model for crystal dissolution. Eur. J. Mineral. 15, 603–615. https://doi.org/10.1127/0935-1221/2003/0015-0603.
Lee, J.B., Kim, Y.J., Kim, K.J., Kim, G.H., Lee, C., Park, Y.D., An, J.C., Yi, H., Oh, K., J., 2025. Il Park, Impact of aspect ratio and crystal size distribution of l-glutamic acid formed by cooling crystallization on drying characteristics. RSC Adv. 15, 83–93. https://doi.org/10.1039/d4ra05935b.
R.J. Leveque, Finite Volume Methods for Hyperbolic Problems, 2002.
J. Li, H. Wang, T. Liu, U. Shakeel, J. Guo, W. Zhu, I.S. Makarov, M.R. Khan, H. Xiao, J. Song, Leveraging topological reactivity of cellulose nanocrystals with 2 allomorph II (CNC-II) to create temperature-sensitive systems for Ibuprofen delivery, n.d. https://ssrn.com/abstract=5119030.
Liang, Z., Zhang, M., Wu, F., Chen, J.F., Xue, C., Zhao, H., 2017. Supersaturation controlled morphology and aspect ratio changes of benzoic acid crystals. Comput. Chem. Eng. 99, 296–303. https://doi.org/10.1016/j.compchemeng.2017.01.010.
I.M. Lifshitz, V. V Slyozov, THE KINETICS OF PRECIPITATION FROM SUPERSATURATED SOLID SOLUTIONS*, 1961.
E. Limpert, W.A. Stahel, M. Abbt, Log-normal Distributions across the Sciences: Keys and Clues, 51 (2001) 341–352. https://doi.org/10.1641/0006.
Liu, G., Wang, Q., Hu, Z., Cai, J., Qin, X., 2019. Maillard-reacted whey protein isolates and epigallocatechin gallate complex enhance the thermal stability of the pickering emulsion delivery of curcumin. J. Agric. Food Chem. 67, 5212–5220. https://doi.org/10.1021/acs.jafc.9b00950.
Lou, F., Ye, L., Kong, M., Yang, Q., Li, G., Huang, Y., 2016. Pickering emulsions stabilized by shape-controlled silica microrods. RSC Adv. 6, 24195–24202. https://doi.org/10.1039/c6ra00360e.
Low, L.E., Tey, B.T., Ong, B.H., Tang, S.Y., 2018. Unravelling pH-responsive behaviour of Fe3O4@CNCs-stabilized Pickering emulsions under the influence of magnetic field. Polymer (Guildf) 141, 93–101. https://doi.org/10.1016/j.polymer.2018.03.001.
Low, L.E., Tan, L.T.H., Goh, B.H., Tey, B.T., Ong, B.H., Tang, S.Y., 2019. Magnetic cellulose nanocrystal stabilized Pickering emulsions for enhanced bioactive release and human colon cancer therapy. Int. J. Biol. Macromol. 127, 76–84. https://doi.org/10.1016/j.ijbiomac.2019.01.037.
Madivala, B., Fransaer, J., Vermant, J., 2009. Self-assembly and rheology of ellipsoidal particles at interfaces. Langmuir 25, 2718–2728. https://doi.org/10.1021/la803554u.
Madivala, B., Vandebril, S., Fransaer, J., Vermant, J., 2009. Exploiting particle shape in solid stabilized emulsions. Soft Matter 5, 1717–1727. https://doi.org/10.1039/b816680c.
Maharana, A., Sehrawat, P., Das, A., Kumar, J., Sarkar, D., 2023. Multi-dimensional population balance modeling of sonocrystallization of pyrazinamide with systematic estimation of kinetic parameters based on uncertainty and sensitivity analyses. Chem. Eng. Res. Des. 200, 356–373. https://doi.org/10.1016/j.cherd.2023.10.049.
Marchisio, D.L., Fox, R.O., 2005. Solution of population balance equations using the direct quadrature method of moments. J. Aerosol. Sci. 36, 43–73. https://doi.org/10.1016/j.jaerosci.2004.07.009.
Marchisio, D.L., Pikturna, J.T., Fox, R.O., Vigil, R.D., Barresi, A.A., 2003. Quadrature method of moments for population-balance equations. AIChE J. 49, 1266–1276. https://doi.org/10.1002/aic.690490517.
Miller, D.J., Henning, T., Grünbein, W., 2001. Phase inversion of W/O emulsions by adding hydrophilic surfactant — a technique for making cosmetics products. Colloids Surf. A Physicochem. Eng. Asp 183–185, 681–688. https://doi.org/10.1016/S0927-7757(01)00494-0.
Mwangi, W.W., Lim, H.P., Low, L.E., Tey, B.T., Chan, E.S., 2020. Food-grade Pickering emulsions for encapsulation and delivery of bioactives. Trends Food Sci. Technol. 100, 320–332. https://doi.org/10.1016/j.tifs.2020.04.020.
A.S. Myerson, D. Erdemir, A.Y. Lee, Handbook of Industrial Crystallization, 2019.
Pickering, S.U., 1907. CXCVI.—Emulsions. J. Chem. Soc. Trans. 91, 2001–2021. https://doi.org/10.1039/CT9079102001.
Pigou, M., Morchain, J., Fede, P., Penet, M.I., Laronze, G., 2018. New developments of the extended quadrature method of moments to solve population balance equations. J. Comput. Phys. 365, 243–268. https://doi.org/10.1016/j.jcp.2018.03.027.
T. Plath, S. Luding, T. Weinhart, Population balance modelling and reconstruction by quadrature method of moments for wet granulation A R T I C L E I N F O, (2024). https://doi.org/10.4121/f5cfe2.
Pohar, A., Likozar, B., 2014. Dissolution, nucleation, crystal growth, crystal aggregation, and particle breakage of amlodipine salts: modeling crystallization kinetics and thermodynamic equilibrium, scale-up, and optimization. Ind. Eng. Chem. Res. 53, 10762–10774. https://doi.org/10.1021/ie501572h.
Qi, F., Wu, J., Sun, G., Nan, F., Ngai, T., Ma, G., 2014. Systematic studies of Pickering emulsions stabilized by uniform-sized PLGA particles: Preparation and stabilization mechanism. J. Mater. Chem. B 2, 7605–7611. https://doi.org/10.1039/c4tb01165a.
Raju, R.R., Liebig, F., Klemke, B., Koetz, J., 2018. pH-responsive magnetic Pickering Janus emulsions. Colloid Polym. Sci. 296, 1039–1046. https://doi.org/10.1007/s00396-018-4321-z.
Ribeiro, A., Lopes, J.C.B., Dias, M.M., Barreiro, M.F., 2023. Pickering emulsions based in inorganic solid particles: from product development to food applications. Molecules 28. https://doi.org/10.3390/molecules28062504.
Röhl, S., Hohl, L., Stock, S., Zhan, M., Kopf, T., von Klitzing, R., Kraume, M., 2023. Application of population balance models in particle-stabilized dispersions. Nanomaterials 13 (4), 698.
Sanyal, S., Huang, H.C., Rege, K., Dai, L.L., 2011. Thermo-responsive core-shell composite nanoparticles synthesized via one-step pickering emulsion polymerization for controlled drug delivery. J. Nanomed. Nanotechnol. 2. https://doi.org/10.4172/2157-7439.1000126.
Shah, B.R., Xu, W., Mráz, J., 2021. Fabrication, stability and rheological properties of zein/chitosan particles stabilized Pickering emulsions with antioxidant activities of the encapsulated vit-D3. Int. J. Biol. Macromol. 191, 803–810. https://doi.org/10.1016/J.IJBIOMAC.2021.09.159.
L.F. Shampine, M.W. Reichelt, S.J. Sci Comput, THE MATLAB ODE SUITE *, 1997. https://epubs.siam.org/terms-privacy.
Shampine, L.F., Reichelt, M.W., Kierzenka, J.A., 1999. Solving index-1 DAEs in MATLAB and simulink. SIAM Rev. 41, 538–552. https://doi.org/10.1137/S003614459933425X.
G. Shan, K. Igarashi, H. Ooshima, Dissolution kinetics of crystals in suspension and its application to l-aspartic acid crystals, 2002.
Shirjandi, M., Haddadi-Asl, V., Abdollahi, E., Khanipour, F., 2022. Synthesis of pH-Sensitive polydopamine capsules via pickering emulsions stabilized by cellulose nanocrystals to study drug release behavior. Polymer (Guildf) 255. https://doi.org/10.1016/j.polymer.2022.125111.

Swapna Reddy, P., Sucharitha, A., Akiti, N., Fenila, F., Sasikumar Jampa, S., 2023. Studies on crystallization process for pharmaceutical compounds using ANN modeling and model based control keywords: solvent selection artificial neural network multi-objective optimization generic model control batch cooling crystallization carbamazepine form III. Digital Chem. Eng. 8, 2772–5081. https://doi.org/10.1016/j.dche.2023.100114.

Szilágyi, B., Nagy, Z.K., 2016. Graphical processing unit (GPU) acceleration for numerical solution of population balance models using high resolution finite volume algorithm. Comput. Chem. Eng. 91, 167–181. https://doi.org/10.1016/j.compchemeng.2016.03.023.

Tang, Q., Xie, X., Li, C., Zhen, B., Cai, X., Zhang, G., Zhou, C., Wang, L., 2019. Medium-chain triglyceride/water Pickering emulsion stabilized by phosphatidylcholine-kaolinite for encapsulation and controlled release of curcumin. Colloids Surf. B Biointerfaces 183. https://doi.org/10.1016/j.colsurfb.2019.110414.

Tikekar, R.V., Pan, Y., Nitin, N., 2013. Fate of curcumin encapsulated in silica nanoparticle stabilized pickering emulsion during storage and simulated digestion. Food Res. Int. 51, 370–377. https://doi.org/10.1016/j.foodres.2012.12.027.

Wood, K., Szewczuk, M.R., Rousseau, D., Neufeld, R.J., 2018. Oseltamivir phosphate released from injectable pickering emulsions over an extended term disables human pancreatic cancer cell survival. Oncotarget 9 (16).

Xia, T., Xue, C., Wei, Z., 2021. Physicochemical characteristics, applications and research trends of edible Pickering emulsions. Trends Food Sci. Technol. 107, 1–15. https://doi.org/10.1016/j.tifs.2020.11.019.

Yang, Y., Fang, Z., Chen, X., Zhang, W., Xie, Y., Chen, Y., Liu, Z., Yuan, W., 2017. An overview of pickering emulsions: Solid-particle materials, classification, morphology, and applications. Front. Pharmacol. 8. https://doi.org/10.3389/fphar.2017.00287.

Zembyla, M., Murray, B.S., Sarkar, A., 2018. Water-in-oil pickering emulsions stabilized by water-insoluble polyphenol. Crystals. https://doi.org/10.1021/acs.langmuir.8b01438.

Zhang, R., Li, B., Wan, L., Zhang, X., Li, L., 2024. Fabrication and characterization of fat crystal-stabilized W/O high internal phase Pickering emulsions (HIPPEs) as a low-fat alternative margarine. LWT 196. https://doi.org/10.1016/j.lwt.2024.115798.

Zhao, X., Huang, B., El-Aooiti, M., Rousseau, D., 2018. Demulsification to control solute release from pickering crystal-stabilized water-in-oil emulsions. J. Colloid Interface Sci. 509, 360–368. https://doi.org/10.1016/j.jcis.2017.08.091.